The North Atlantic Oscillation in the NCEP–NCAR Reanalysis

STEFAN HASTENRATH AND LAWRENCE GREISCHAR

Department of Atmospheric and Oceanic Sciences, University of Wisconsin—Madison, Madison, Wisconsin

(Manuscript received 22 June 2000, in final form 28 September 2000)

ABSTRACT

The upper-air circulation characteristics of the North Atlantic oscillation (NAO) are studied from the 1958–97 National Centers for Environmental Prediction–National Center for Atmospheric Research reanalysis, with regard to interannual variability and long-term trends. The low (high) phase of the NAO is defined by small (large) values of the Ponta Delgada, Azores, minus Akureyri, Iceland, surface pressure difference. For the fields of 200-mb topography, divergence, and divergent flow; 500-mb vertical motion; 1000-mb topography and total wind; and SST during January, differences are computed between ensembles of years of extremely low- minus high-NAO phase and are tested for statistical significance. In the low-NAO phase, topographies throughout the tropospheric column stand anomalously high (low) in the subpolar (subtropical) domains. Ascending motion and upper-tropospheric divergent outflow from the realm of the Icelandic low broadly southward, and convergent inflow and subsidence on the poleward side of the Azores high, are reduced. These vertical motion departures support the raised (lowered) 1000-mb topography in the subpolar (subtropical) domains. The weakened subtropical high entails slower trade winds that through reduced evaporation and wind stirring are conducive to warmer sea surface and slower midlatitude westerlies that through reduced Ekman transport lead to colder waters on the poleward side of the anticyclonic axis. Similarly, the weakened cyclonic circulation around the Icelandic low, through reduced Ekman transport, makes for a warmer sea surface. These SST departures are imparted to the overlying atmosphere. Long-term evolutions in the patterns of upper-tropospheric divergence and divergent flow, midtropospheric vertical motion, and SST accompany the trends in 1000-mb topography toward greater prevalence of the high-NAO phase.

1. Introduction

The pioneering work of Hildebrandsson (1897) on the atmospheric centers of action provided the basis for Walker's (1924) concept of the North Atlantic oscillation (NAO), which he viewed in context with two other systems of low-frequency inverse pressure variations, namely, the Southern Oscillation (SO) and the North Pacific oscillation (reviews in Hastenrath 1985, 253–257; Lamb and Peppler 1987). The NAO is a pressure seesaw between the Azores high and the Icelandic low and is most prominent in boreal winter. With strong Azores high and Icelandic low, the surface westerlies over the Atlantic are well developed, and this results in mild winters in western Europe, anomalously wet in the north and dry in the south. The role of the NAO for the interannual variability of the surface climate in the Atlantic–European sector has been discussed in a series of papers (van Loon and Rogers 1978; Rogers and van Loon 1979; Rogers 1984, 1985, 1990; Meehl and van Loon 1979; Malberg and Bökens 1993; Malberg and Frattesi 1995; Hurrell 1995; Blender et al. 1997; Xie and Tanimoto 1998; Machel et al. 1998; Kapala et al. 1998), and Lamb and Peppler (1987) studied the implications for the rainfall of Morocco. By contrast, the exploration of the atmospheric circulation mechanisms involved has been more limited and mostly very recent (Barnston and Livezey 1987; Deser and Blackmon 1993; Hurrell and van Loon 1997; Rodwell et al. 1999; Thompson and Wallace 1998, 2000a, b; Wallace 2000).

The National Centers for Environmental Prediction–National Center for Atmospheric Research (NCEP–NCAR) reanalysis (Kalnay et al. 1996) has opened new prospects for ascertaining the upper-air characteristics of the NAO. While based on the model assimilation of observations, it is an internally consistent system, and the 40-yr record allows a generous sampling of contrasting extreme phases of the NAO. The NCEP–NCAR reanalysis is the essential data source for the present study. Data and analysis are described in sections 2 and 3; the long-term mean circulation is documented in section 4, as background for the analysis of the NAO upper-air patterns in sections 5 and 6; and a synthesis is offered in the closing section 7.

Corresponding author address: Stefan Hastenrath, Department of Atmospheric and Ocean Sciences, University of Wisconsin—Madison, 1225 West Dayton St., Madison, WI 53706.
E-mail: barafu@macc.wisc.edu

2. Data and analysis

The main data source for this study was the NCEP–NCAR reanalysis (Kalnay et al. 1996; Kousky and Ropelewski 1997) at a 2.5° lat–long resolution for the years 1958–97. Data were processed into individual monthly mean fields. Of particular interest here are the fields of topography, wind and vertical velocity, and the levels 200, 500, and 1000 mb.

From the total wind field at selected levels velocity potential and streamfunction were computed as described in Mancuso (1967), Krishnamurti (1971), and Krishnamurti et al. (1973), with full coverage from 75°N to 75°S and a grid spacing of 2.5°. An inner subdomain from these near-global fields is used here. From the fields of velocity potential maps were then constructed of divergent wind component and divergence.

Ship observations of sea surface temperature (SST) and surface pressure and wind were available in the Comprehensive Ocean–Atmosphere Data Set (COADS) collection, with spatial resolution of 2° squares (Woodruff et al. 1987).

The long-term series at two barometric stations served to compile a circulation index, as described in section 3.

3. North Atlantic oscillation index

The NAO may be defined by the difference in pressure at Ponta Delgada, Azores, minus that at Akureyri, Iceland (Rogers 1984, 1985). Time series plots of this index are presented in Fig. 1 for the months of January, April, July, and October. The location of the two pressure stations is indicated in Fig. 2d. The low phase of the NAO is defined by anomalously low pressure at Ponta Delgada and high pressure at Akureyri. From the Ponta Delgada minus Akureyri pressure index the 10 most extreme years of the low and high phases were selected for the cardinal months January, April, July, and October. These are listed in Table 1. The 10 most extreme years for the low and high phases of the NAO are marked in Fig. 1.

Figure 1 shows that the NAO index as defined here in accordance with earlier work (Rogers 1984, 1985) is overall largest in January, and smallest in July and October. January also exhibits by far the largest interannual and long-term variability, although the difference between the ensembles of the 10 yr with the highest and lowest values of NAO index is statistically significant at the 1% level, according to a *t* test, for all four months. That the NAO as defined here is well developed in the boreal winter is known from earlier work, and the analysis in later sections shall accordingly focus on the January core of the boreal winter. In a related vein, the long-term trend toward larger NAO values is statistically significant for January, but not the other months. However, given the seasonal shifts of the centers of action, patterns related to NAO persist through much of the year (Barnston and Livezey 1987).

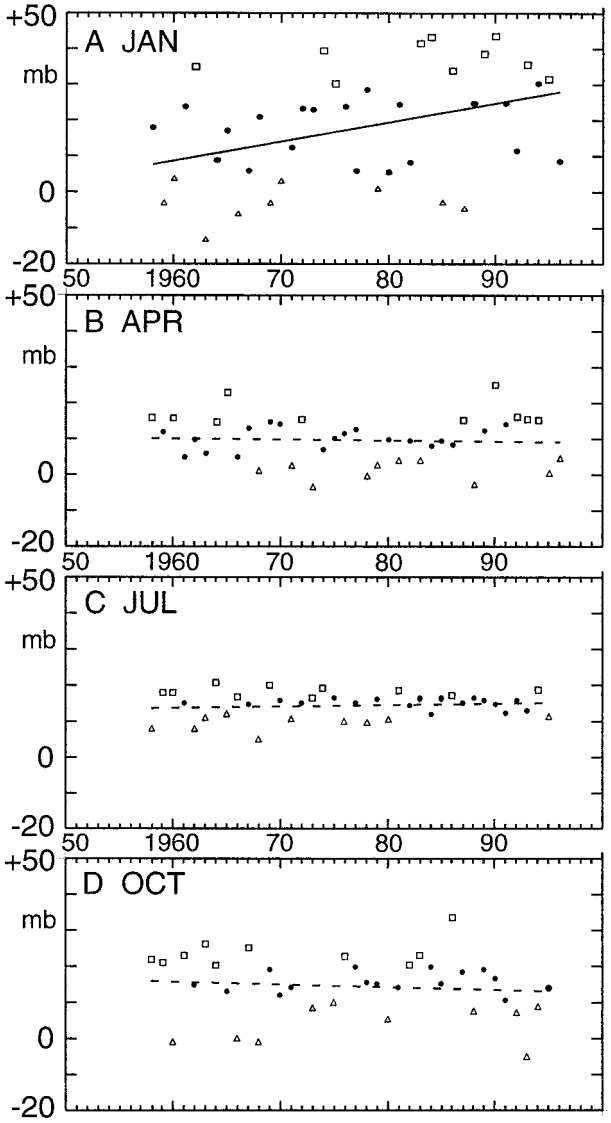

FIG. 1. Time series plots of the Ponta Delgada − Akureyri pressure index (mb) for the period 1958–96. Trends significant at the 5% level are shown by solid lines, other trends by dashed lines. Open squares indicate the 10 yr of highest and open triangles the 10 yr of lowest NAO index: (a) Jan, (b) Apr, (c) Jul, (d) Oct.

In order to explore the NAO index in relation to large-scale variability, correlation matrices were calculated (not presented here), for all four months, between the pressure at Ponta Delgada (P) and Akureyri (A), the NAO index (P − A), the pressure at Tahiti (T), and Darwin (D), and the SO index (T − D). Apart from the trivial significant correlations (such as P − A with P and A, T − D with T and D), the following results are of interest; significant negative correlations are reached between P and D in October, January, and April, and between T and D in the austral winter months July and October; while P − A and T − D are uncorrelated all year round, thus offering no support to a linkage be-

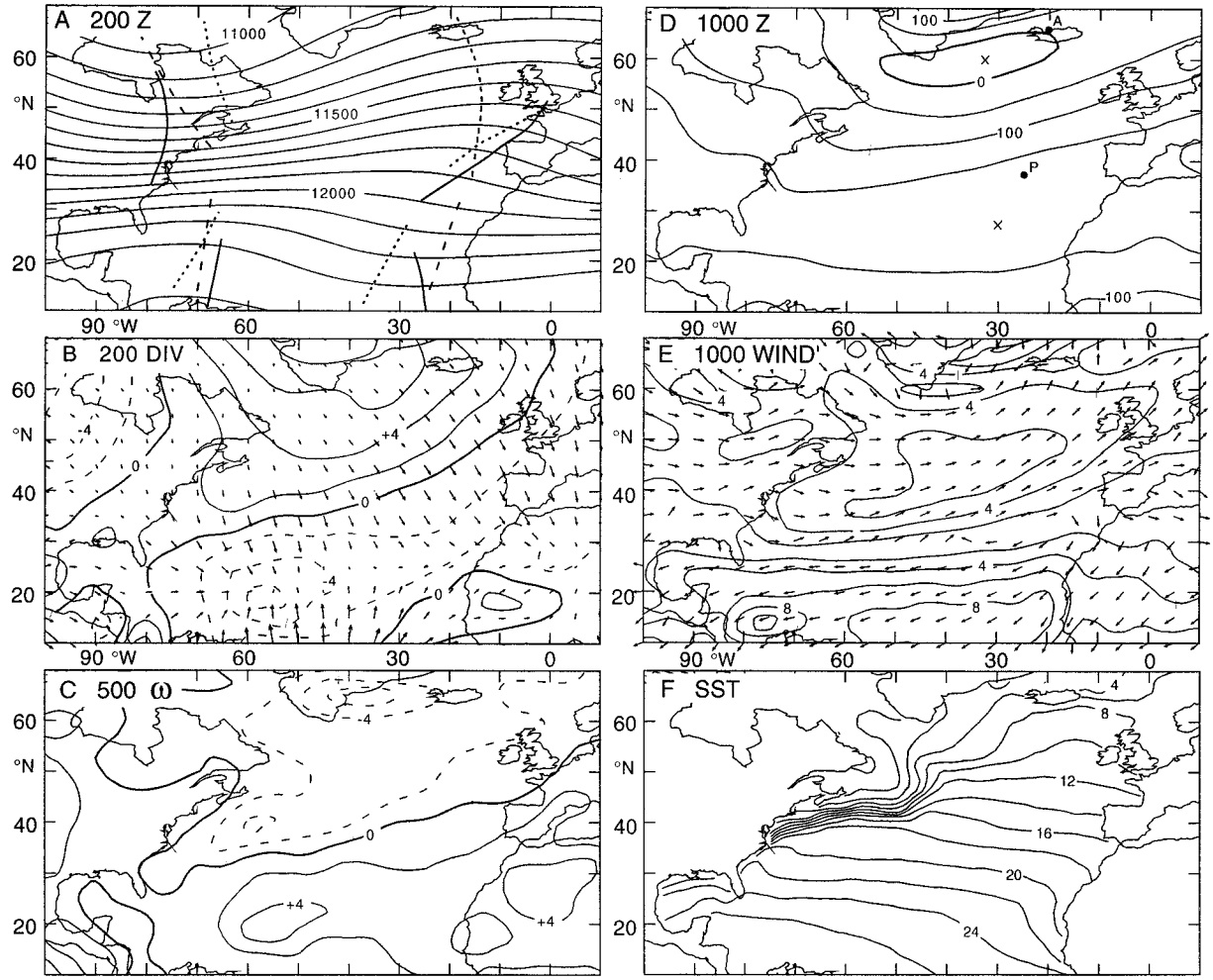

FIG. 2. Maps of Jan 1958–97 mean circulation. (a) The 200-mb topography, with isoline spacing of 100 gpm. Trough and ridge positions are marked by solid lines for the long-term mean, by dashed lines for the ensemble of 10 yr of low-NAO phase and by dotted lines for the ensemble of 10 yr of high-NAO phase. (b) The 200-mb divergence and divergent wind component. For divergence isoline spacing is 2×10^{-6} s^{-1}, with dashed lines indicating negative values. For the divergent wind component, arrow length of 1° lat corresponds to 1 m s^{-1}. (c) The 500-mb omega vertical motion, with isoline spacing of 2×10^{-4} mb s^{-1} and dashed lines indicating negative values or upward motion. (d) The 1000-mb topography, with isoline spacing of 50 gpm. Crosses indicate the core of the subpolar low and subtropical high. Dots denote the location of the surface pressure stations Ponta Delgada (P) and Akureyri (A). (e) The 1000-mb total wind, with isotach spacing of 2 m s^{-1}. (f) The sea surface temperature, with isoline spacing of 2°C.

tween NAO and SO. This exploration thus complements Rogers's (1984) report of a lack of associations between the two oscillation systems.

4. Background circulation

The 1958–97 mean circulation in the North Atlantic sector is presented in Figs. 2a–d, for the January core of the boreal winter by maps of the 200-mb topography (Fig. 2a), 200-mb divergence and divergent wind component (Fig. 2b), 500-mb omega vertical motion (Fig. 2c), and 1000-mb topography (Fig. 2d). This documentation serves as a background reference for the discussion, in sections 5 and 6, of interannual variability and long-term trends related to the North Atlantic oscillation.

The January map of the upper-tropospheric contour field (Fig. 2a) shows in the higher latitudes a trough over the western and a ridge over the eastern Atlantic, and in the Tropics an approximately opposite wave pattern. The map of upper-tropospheric divergence and divergent wind component (Fig. 2b) features vigorous divergent outflow from the northern part of the Atlantic southeastward into a broad band of strong convergent inflow stretching from northern South America to Europe. Given the typical poleward decrease of tropopause height, it is recognized that the 200-mb surface (Figs. 2a and 2b) represents the upper troposphere well in the lower but not the higher latitudes. Complementary analyses for 500 mb (not reproduced here) offer plausible vertical coherence, but patterns are less pronounced and less consistent with the field of vertical motion. Indeed

TABLE 1. Years of extremely low and high phases of the NAO.

Jan	Apr	Jul	Oct
Low			
1959	1968	1958	1960
1960	1971	1962	1966
1963	1973	1963	1968
1966	1978	1965	1973
1969	1979	1968	1975
1970	1981	1971	1980
1979	1983	1976	1988
1980	1988	1978	1992
1985	1995	1980	1993
1987	1996	1995	1994
High			
1962	1958	1959	1958
1974	1960	1960	1959
1975	1964	1964	1961
1983	1965	1966	1963
1984	1972	1969	1964
1986	1987	1973	1967
1989	1990	1974	1976
1990	1992	1981	1982
1993	1993	1986	1983
1995	1994	1994	1986

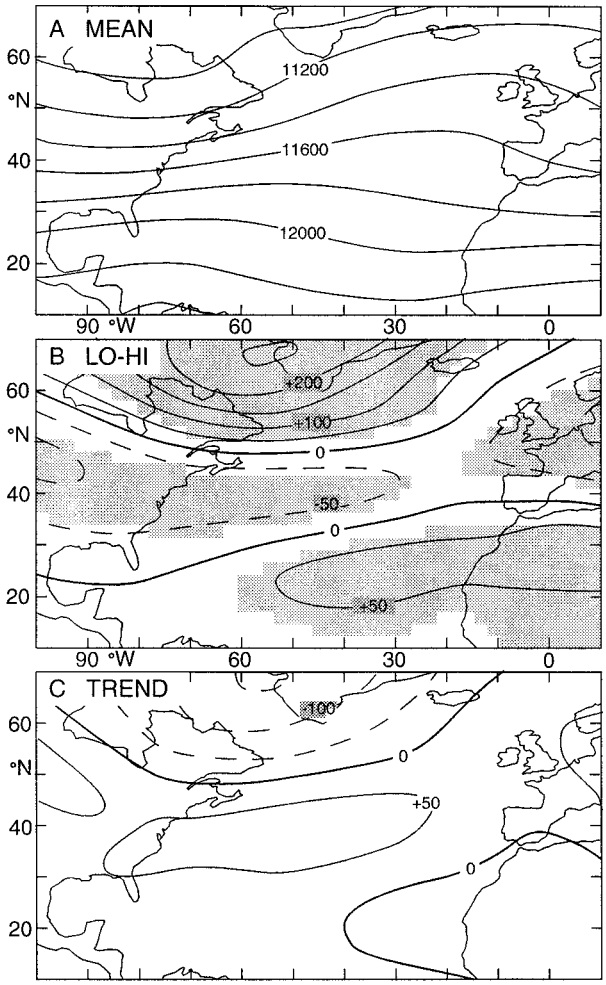

FIG. 3. Maps of Jan 200–1000-mb thickness. (a) The 1958–97 mean with isoline spacing of 200 gpm. (b) Differences of the ensembles of the 10 yr of highest values of NAO pressure index, with isoline spacing of 50 gpm. (c) Trends expressed as the difference of the 1997 minus 1958 values on a linear trend line, with isoline spacing of 50 gpm. In (a) and (b), dashed lines indicate negative values, and statistical significance at the 5% level is indicated by shading.

the map of midtropospheric vertical motion (Fig. 2c) should be appreciated in context with the upper-tropospheric divergence pattern. Thus, ascending motion prevails in the northern part of the map area, contrasting with strong subsidence over the low-latitude Atlantic. The map of 1000-mb topography (Fig. 2d), shows the Icelandic low broadly concordant with the core of ascending motion and the Azores high under the aforementioned strong subsidence (Fig. 2c). Most prominent in the 1000-mb wind field (Fig. 2e) is the anticyclonic flow around the Azores high and the cyclonic circulation around the Icelandic low. Consistent with the 1000-mb contour and wind patterns from the NCEP–NCAR dataset (Figs. 2d and 2e) are the analyses of the ship observations of surface pressure and wind from COADS (not reproduced here). In addition to the overall northward temperature decrease, the SST map (Fig. 2f) reflects the signature of the Gulf Stream and the Labrador and Canary Currents. Broadly concordant with the basinwide SST pattern (Fig. 2f) is the tropospheric thickness pattern (Fig. 3a) reflecting the tropospheric mean temperature. From the comparison of Figs. 2a and 2d and 3a it is seen that the 200-mb absolute topography is largely controlled by the 200-mb over 1000-mb thickness pattern, or tropospheric mean temperature.

April (not shown here) has circulation patterns similar to but less pronounced than for January (Fig. 2). In particular, the midtropospheric ascending motion and upper-tropospheric divergence over the northern North Atlantic is weaker, as are the upper-tropospheric convergence and midtropospheric subsidence in the low latitudes, where moreover the centers of largest action appear shifted eastward. The July and October patterns differ substantially from those of January and April, most notable being the relatively weak subsidence over the low-latitude Atlantic.

5. North Atlantic oscillation patterns

With the background of the long-term average January conditions portrayed in Figs. 2 and 3a the present section explores the characteristics of upper-air circulation for ensembles of years with extremely low versus high NAO index. Figure 4 showing the differences of the low minus the high ensembles essentially reflects the patterns characteristic of the low years.

It seems appropriate to begin with the map of 1000-mb topography (Fig. 4d), representative of the near-surface pressure, because the NAO has traditionally

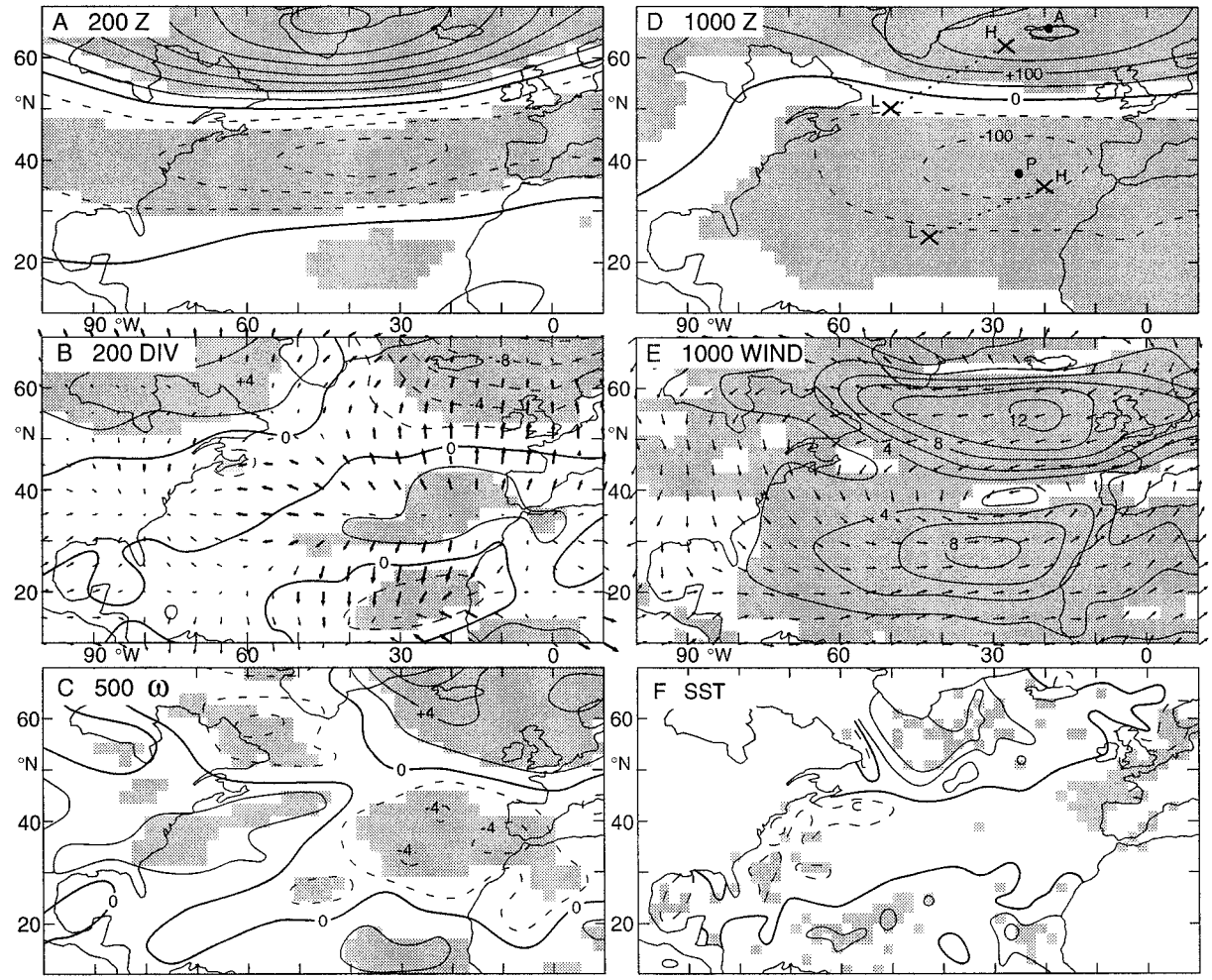

FIG. 4. Maps of Jan differences of the ensembles of the 10 yr of lowest minus the 10 yr of highest values of the NAO pressure index. Dashed lines denote negative values, and shading and bold arrows indicate significance at the 5% level according to a *t* test. (a) The 200-mb topography, with isoline spacing of 50 gpm. (b) The 200-mb divergence with isoline spacing of 2×10^{-6} s^{-1}, and divergent wind component with wind arrow length of 2° lat corresponding to 1 m s^{-1}. (c) The 500-mb omega vertical motion, with isoline spacing of 2×10^{-4} mb s^{-1}. (d) The 1000-mb topography, with isoline spacing of 50 gpm. Crosses and dotted lines indicate the core of the subpolar low and subtropical high during the low (L) and high (H) phases of the NAO. Dots denote the location of the surface pressure stations Ponta Delgada (P) and Akureyi (A). (e) 1000-mb total wind, with isotach spacing 2 m s^{-1}. (f) Sea surface temperature, with isoline spacing of 0.5°C.

(Walker 1924; Rogers 1984, 1985) been described in terms of the large-scale patterns of the variations in surface pressure. Figure 4d exhibits major consistency with earlier work (e.g., Rogers 1984). Statistical significance is reached in most of the map area. Differences are positive over the northern North Atlantic with largest values around Iceland, contrasting with negative differences farther south and with largest values in the band 30°–50°N across the Atlantic. With reference to the long-term mean map (Fig. 2d), this entails slackened meridional pressure gradients on both the equatorward and poleward sides of the weakened and southward displaced North Atlantic high and, consistent with Roger's (1990) findings, a weakened and southwestward displaced Icelandic low. Directly related to the 1000-mb topography (Fig. 4d) is the 1000-mb total wind field (Fig. 4e). Thus, accompanying the slackened meridional pressure gradients, the trades and the midlatitude westerlies are weakened, as is the cyclonic circulation around the Icelandic low. In particular, a difference maximum near 30°N reflects the southward displacement of the high pressure axis; another difference maximum at about 50°–60°N is at the northern edge of the long-term mean midlatitude westerlies; while the difference minimum is located in the core of the westerlies (Figs. 2d,e and 4d,e). As further part of the contrasts of the low versus the high NAO phase, the airstream from the Atantic is more nearly zonal and pointed toward more southerly parts of Europe, reminiscent of patterns described by Rogers (1990), Hurrell (1995), and Blender et al.

(1997). Consistent with the 1000-mb contour and wind difference patterns from the NCEP–NCAR dataset (Figs. 4d and 4e) are the analyses of the ship observations of surface pressure and wind from COADS (not reproduced here).

The map of wind differences (Fig. 4e) is pertinent to that of SST (Fig. 4f). Thus, the weakened trade winds imply reduced evaporation and wind stirring, conducive to warmer sea surface, consistent with the warm differences equatorward of about 30°N. Poleward of the anticyclonic axis, the slower midlatitude westerlies entail weaker southward and convergent Ekman transport, resulting in diminished downwelling and thus favoring cooler surface conditions. In a similar vein, the weakened cyclonic wind stress around the Icelandic low translates into smaller outward directed Ekman transport and upwelling, conducive to warmer surface waters. The SST pattern, in turn, appears imprinted on the thermal structure of the overlying atmosphere, as may be appreciated from a comparison of Figs. 4f and 3b. Thus the band of negative SST differences extending at about 30°–50°N from North America across the Atlantic to the coasts of western and northwestern Europe is overlain by a strip of significant negative differences in tropospheric thickness; and the positive SST differences in the adjacent areas of the tropical and subpolar Atlantic, respectively, find their correspondence in significant positive thickness differences. Working on atmosphere–ocean interactions on shorter than monthly timescales, Deser and Timlin (1997) commented favorably on the quality of the NCEP–NCAR dataset.

The upper-air maps (Figs. 4a, b, c) may shed light on the origin of the NAO near-surface pressure pattern illustrated in Fig. 4d. Of immediate interest is the field of vertical motion, so Fig. 4c should be compared to Fig. 4d. Note that in Fig. 4c positive differences indicate enhanced subsidence or reduced ascending motion in the low NAO phase. Figure 4c shows significant negative differences in the realm of largest negative 1000-mb differences on the poleward side of the North Atlantic high (Figs. 2d and 4d), and significant positive differences over the northern North Atlantic, with largest values near Iceland, where the positive 1000-mb differences indicate a weakened Icelandic low during the low NAO phase. Indeed, overall in the regions with statistical significance the differences in Figs. 4c and 4d tend to be of the same sign, indicating a tendency in the sense of increased (decreased) surface pressure to be associated with enhanced (reduced) subsidence or reduced (enhanced) ascending motion.

Next compare the differences in midtropospheric vertical motion (Fig. 4c) to those of upper-tropospheric divergence and divergent flow (Figs. 4b and 2b). Most conspicuous is the coincidence of significantly reduced upper-tropospheric divergence (Figs. 4b and 2b) with significantly reduced ascending motion (Fig. 4c) in the realm of the Icelandic low, and significantly reduced upper-tropospheric convergence and subsidence (Figs. 4b, c and 2b, c) on the poleward side of the North Atlantic high. Overall, the differences in midtropospheric vertical motion and in upper-tropospheric divergence are of opposite sign, as plausible from mass continuity. Figure 4b further shows the correspondence between the differences in the patterns of divergent flow and divergence; particularly prominent being the reduced divergent outflow from the northern North Atlantic southward and southeastward, and the reduced convergent inflow to the upper troposphere over the poleward flank of the North Atlantic high (Figs. 4b, 2b, and 2d). Complementary analyses for 500 mb (not reproduced here) offer continuity in the vertical, but patterns are less pronounced and less consistent with the field of large-scale vertical motion than Fig. 4b.

The map of upper-tropospheric topography (Fig. 4a) shows a zonal arrangement strikingly similar to those of SST (Fig. 4f) and of 1000-mb topography (Fig. 4d); namely, small positive differences equatorward of about 30°N, large negative differences in the band 30°–50°N, and very large positive differences further poleward. The maps of upper-tropospheric topography during the low and high phases of the NAO (not reproduced here), from which Fig. 4a was constructed, show some differences in the midlatitude long-wave pattern from the long-term mean conditions (Fig. 2a). In conjunction, Figs. 3b and 4a,d,e, and 4f, indicate that the NAO-related changes in the topography are prevailingly barotropic, being of the same sign from the upper to the lower troposphere; that the wind stress pattern controlled by the near-surface pressure changes produces changes of SST, with the realm of the midlatitude westerlies having a sign opposite to that in the trade wind belt and in the cyclonic wind regime around the Icelandic low; and that the changes in SST are imprinted on the layer-mean temperature of the overlying atmosphere. Very recent work (Thompson and Wallace 2000a,b; Wallace 2000) opens perspectives on the mechanisms leading to the changes in the upper-tropospheric topography pattern, and the ways in which the topography affects the fields of divergence and divergent flow in the upper troposphere.

6. Trends

Long-term changes in the winter climate of the North Atlantic and Europe related to the NAO have been discussed previously based on surface observations (reviews in Rogers 1985; Hurrell 1995; Hurrell and van Loon 1997). The NCEP–NCAR dataset offers the possibility to examine such evolutions in the context of the upper-air circulation. To that end, Fig. 5 presents maps of long-term trends in pertinent fields and should be appreciated with reference to the corollary Fig. 2.

The map of 1000-mb topography (Fig. 5d) shows largest negative differences around Iceland, and largest positive values in the band 30°–50°N across the Atlantic, with statistical significance reached in key areas. This

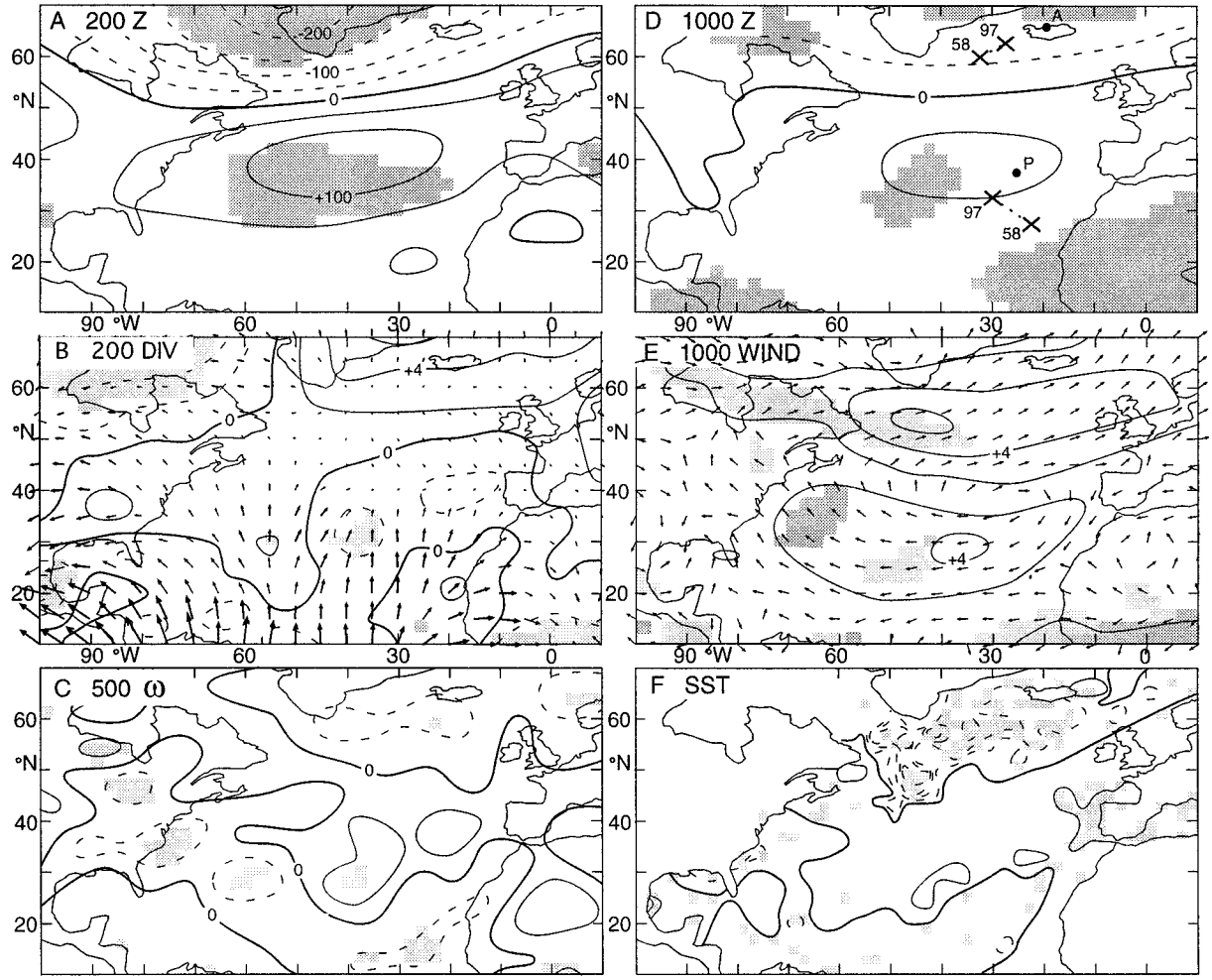

FIG. 5. Maps of Jan trends 1958–97, expressed as the difference of the 1997 − 1958 values on a linear trend line. Dashed lines denote negative values and shading and bold arrows indicate significance at the 5% level. (a) The 200-mb topography, with isoline spacing of 50 gpm. (b) The 200-mb divergence with isoline spacing of 2×10^{-6} s^{-1}, and divergent wind component with arrow length of 2° lat corresponding to 1 m s^{-1}. (c) The 500-mb omega vertical motion, with isoline spacing of 2×10^{-4} mb s^{-1}. (d) The 1000-mb topography, with isoline spacing of 50 gpm. Crosses and dotted lines indicate the core of the subpolar low and subtropical high at beginning (1958) and end (1997) of the 1958–97 record. Dots denote the location of the surface pressure stations Ponta Delgada (P) and Akureyri (A). (e) The 1000-mb total wind, with isotach spacing of 2 m s^{-1}. (f) Sea surface temperature, with isoline spacing of 0.5°C.

corresponds to a trend toward a more prevalent high-NAO phase, as illustrated also in the time series plot in Fig. 1a. Based on a different data source and analysis approach and for the period 1960–90, Malberg and Bökens (1993) arrived at a similar conclusion. In accordance with the mapped 1000-mb topography (Fig. 5d), the 1000-mb total wind (Fig. 5e) reflects accelerating trade winds and midlatitude westerlies and increasing cyclonic flow around the Icelandic low, although statistical significance is reached only in limited areas. Consistent with the changing wind stress forcing (Fig. 5e), there is cooling equatorward of about 30°N, warming at 30°–50°N, and cooling farther poleward (Fig. 5f). Hugging the coast of Europe, the band of warming extends to the subpolar latitudes. This pattern detail has also been depicted by Malberg and Frattesi (1995) for the period 1973–92. The pattern of SST trends (Fig. 5f) is also reflected in the trends of tropospheric mean temperature or thickness (Fig. 3c). Thus, a band of most strongly increasing thickness extends from North America across the Atlantic to western and northwestern Europe, broadly concordant with the swath exhibiting oceanic warming; and the surface cooling in the northwestern Atlantic is matched by decreasing tropospheric thickness.

For the upper-air maps, Fig. 5c exhibits increasing subsidence on the poleward side of the North Atlantic high and increasing upward motion around Iceland (Fig. 2d), although statistical significance is reached only in limited areas. Consistent with the evolution of vertical motion (Fig. 5c), there is increasing upper-tropospheric

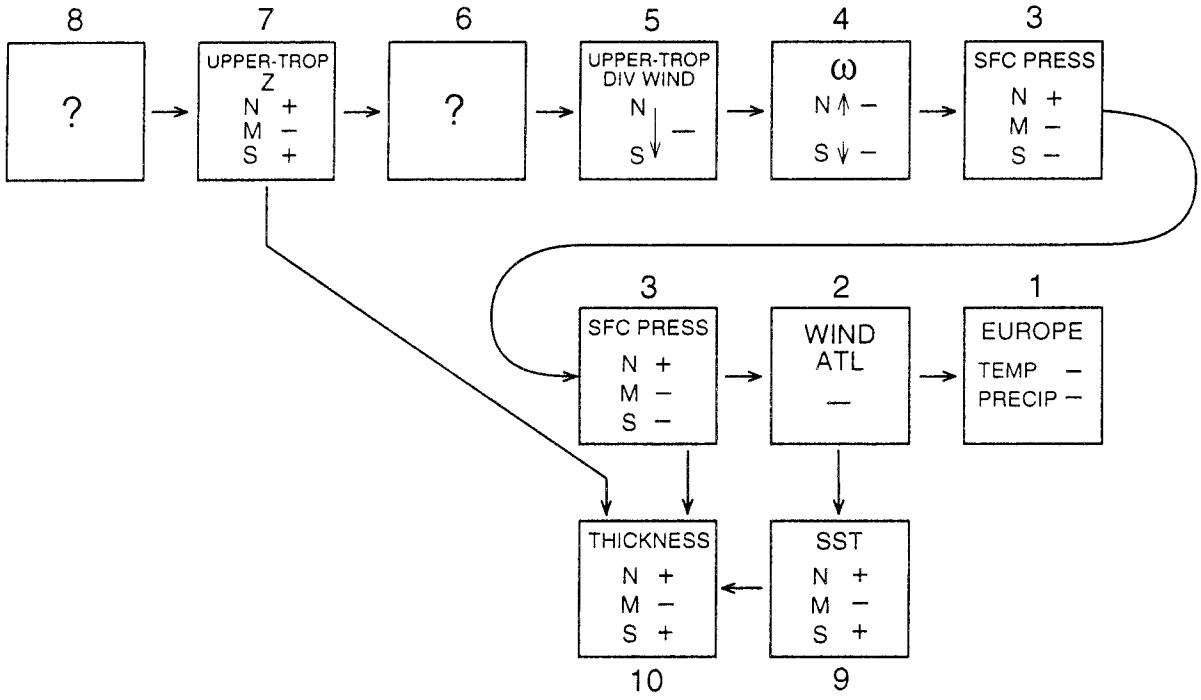

FIG. 6. Schematic diagram of mechanisms in the North Atlantic oscillation, representative of the low-NAO phase. Here N, M, and S denote north, midlatitudes, and south, respectively. The middle part of the diagram (boxes 1–3) represents the causality chain ascertained in earlier work, while the upper (boxes 3–8) and the lower part (boxes 9–10) pertain to findings of the present study: (1) Europe winter temperature and precipitation, (2) surface wind over the Atlantic, (3) meridional gradient of surface pressure over the Atlantic, (4) vertical motion in Iceland and Azores domains, (5) Upper-tropospheric southward directed divergent to convergent outflow, (6) Circulation mechanism needing further exploration, (7) Upper-tropospheric topography, (8) Circulation mechanism needing further exploration, (9) sea surface temperature pattern, and (10) tropospheric thickness pattern.

divergence and divergent outflow from the realm of the Icelandic low and of convergent inflow to the atmospheric column over the poleward side of the North Atlantic high (Figs. 5b and 2d), although statistical significance is reached only in limited areas. Complementary analyses for 500 mb (not reproduced here) offer continuity in the vertical but are less consistent with the field of large-scale vertical motion than Fig. 5b. The map of upper-tropospheric topography (Fig. 5a) shows zonal arrangements similar to those of SST (Fig. 5f) and of 1000-mb topography (Fig. 5d), with trends overall stronger for the 200-mb (Fig. 5a) than for the 1000-mb level (Fig. 5d); statistical significance is reached in extended areas (Fig. 5a). Accordingly, Fig. 3c reveals correspondingly strong trends in the tropospheric thickness, with statistical significance in key regions.

Overall, the maps in Fig. 5 appear broadly inverse to the corresponding ones in Fig. 4 an evolution toward greater prevalence of the high NAO phase, with mutually coherent trends in the large-scale circulation setting.

7. Conclusions

The North Atlantic oscillation has recurrently been the subject of investigations throughout much of the past century. Manifestations of the NAO are prominent in the near-surface pressure pattern, and through the lower-tropospheric flow it has a powerful impact on the winter surface climate of Europe and North Africa.

The NCEP–NCAR 40-Year Reanalysis invited an exploration of upper-air circulation mechanisms operative in the NAO. Drawing on the Ponta Delgada minus Akureyri pressure index, and in confirmation of earlier work, the NAO was found to be confined to the boreal winter and unrelated to the SO. Work was therefore directed to January, and analysis included the fields of 200-mb topography, divergence and divergent flow, 500-mb vertical motion, 1000-mb topography and total wind, and SST. Differences were computed between ensembles of years of extremely low- minus high-NAO phase and tested for statistical significance. The investigation shed light on some upper-air mechanisms involved. A chain of causalities is schematically indicated in Fig. 6, with reference to the low-NAO phase. That the winter temperature and precipitation of Europe and North Africa are affected by the westerlies, which in turn are controlled by the meridional pressure gradient in the Atlantic sector, is known from earlier work (boxes 1–3 in Fig. 6). The present research then aimed at the upper-air mechanisms controlling the meridional gradient of surface pressure (boxes 3–10 in Fig. 6).

In the low phase of the NAO, both the 200- and 1000-mb topographies stand anomalously high around the Icelandic low and low on the poleward flank of the Azores high (box 7 in Fig. 6). Ascending motion and upper-tropospheric divergent outflow from the realm of the Icelandic low and the convergent inflow and subsidence on the poleward side of the Azores high are reduced (boxes 5–4 in Fig. 6). These vertical motion departures support the raised 1000-mb topography around the Icelandic low and the convergent inflow and subsidence on the poleward side of the Azores high (boxes 4–3 in Fig. 6). Regarding the relation of upper-tropospheric divergence and divergent flow to the topography pattern and the mechanisms leading to changes in the topography pattern, the recent works of Thompson and Wallace (2000a,b) and Wallace (2000) may open pertinent perspectives. Wallace (2000) in particular argues that the NAO should be appreciated in a hemispheric context.

Vertical motion appears to control the departures in 1000-mb topography (boxes 4–3 in Fig. 6), but in a separate vein a control on the tropospheric thickness pattern can be appreciated (boxes 3–2–9–10 in Fig. 6). Thus, in the low-NAO phase, along with the weakened Azores high and Icelandic low, the trade winds, midlatitude westerlies, and cyclonic circulation over the northern North Atlantic are slower; reduced evaporation and wind stirring are conducive to a warmer upper ocean in the trade wind belt, and diminished Ekman transport favors cold departures in the midlatitudes and warm departures under the subpolar low. Such a zonal arrangement of warm–cold–warm departures of SST is reflected in the layer-mean temperature of the overlying atmosphere, or the thickness pattern. Thus, in the low-NAO phase around the Icelandic low, surface pressure is anomalously high with a warm troposphere, while on the poleward flank of the Azores high, surface pressure is anomalously low with a cold troposphere (boxes 3 and 10 in Fig. 6). Long-term evolutions in upper-air circulation, near-surface wind pattern, and SST over the recent 40-yr period are in tune with a trend toward greater prevalence of the high-NAO phase.

Acknowledgments. This study was supported by NSF Grant ATM-9732673. We thank the anonymous reviewers for comments on an earlier version of this paper.

REFERENCES

Barnston, A. G., and R. E. Livezey, 1987: Classification, seasonality and persistence of low-frequency atmospheric circulation patterns. *Mon. Wea. Rev.,* **115,** 1083–1126.

Blender, R., K. Fraedrich, and F. Lunkeit, 1997: Identification of cyclone-track regimes in the North Atlantic. *Quart. J. Roy. Meteor. Soc.,* **123A,** 727–741.

Deser, C., and M. L. Blackmon, 1993: Surface climate variations over the North Atlantic Ocean during winter: 1900–1989. *J. Climate,* **6,** 1743–1753.

——, and M. S. Timlin, 1997: Atmospheric–ocean interaction on weekly timescales in the North Atlantic and Pacific. *J. Climate,* **10,** 393–408.

Hastenrath, S., 1985: *Climate and Circulation of the Tropics.* Reidel, 455 pp.

Hildebrandsson, H., 1897: Les centres d'action de l'atmosphère. *Kongliga Svenska Vetenskaps-Akademiens Handlingar,* Vol. 29, 36 pp.

Hurrell, J., 1995: Decadal trends in the NAO: Regional temperature and precipitation. *Science,* **269,** 676–679.

——, and H. van Loon, 1997: Decadal variations in climate associated with the North Atlantic oscillation. *Climatic Change,* **36,** 301–326.

Kalnay, E., and Coauthors, 1996: The NCEP/NCAR 40-Year Reanalysis Project. *Bull. Amer. Meteor. Soc.,* **77,** 437–471.

Kapala, A., H. Machel, and H. Flohn, 1998: Behaviour of the centres of action above the Atlantic since 1881: Part II: Associations with regional climate anomalies. *Int. J. Climatol.,* **18,** 23–36.

Kousky, V. E., and C. F. Ropelewski, 1997: *The Tropospheric Seasonally Varying Mean Climate over the Western Hemisphere (1979–1995).* NCEP/Climate Prediction Center, Atlas No. 3, 135 pp.

Krishnamurti, T. N., 1971: Tropical east–west circulations during the northern summer. *J. Atmos. Sci.,* **28,** 1342–1347.

——, M. Kanamitsu, W. J. Koss, and J. D. Lee, 1973: Tropical east–west circulations during the northern winter. *J. Atmos. Sci.,* **30,** 780–787.

Lamb, P. J., and R. A. Peppler, 1987: North Atlantic oscillation: Concept and an application. *Bull. Amer. Meteor. Soc.,* **68,** 1218–1225.

Machel, H., A. Kapala, and H. Flohn, 1998: Behaviour of the centres of action above the Atlantic since 1881. Part I: Characteristics of seasonal and interannual variability. *Int. J. Climatol.,* **18,** 1–22.

Malberg, H., and G. Bökens, 1993: Changes in the pressure-, geopotential-, and temperature fields between the subtropics and the subpolar region over the Atlantic in the period 1960–90. *Meteor. Z.,* **2,** 131–137.

——, and G. Frattesi, 1995: Changes of the North Atlantic sea surface temperature related to the atmospheric circulation in the period 1973 to 1992. *Meteor. Z.,* **4,** 37–42.

Mancuso, R. L., 1967: A numerical procedure for computing fields of streamfunction and velocity potential. *J. Appl. Meteor.,* **6,** 994–1001.

Meehl, G. A., and H. van Loon, 1979: The seesaw in winter temperatures between Greenland and northern Europe. Part III: Teleconnections with lower latitudes. *Mon. Wea. Rev.,* **107,** 1095–1106.

Rodwell, M. J., D. P. Rowell, and C. K. Folland, 1999: Oceanic forcing of wintertime North Atlantic oscillation. *Climatic Change,* **36,** 301–326.

Rogers, J. C., 1984: The association between the North Atlantic oscillation and the Southern Oscillation in the Northern Hemisphere. *Mon. Wea. Rev.,* **112,** 1999–2015.

——, 1985: Atmospheric circulation changes associated with the warming over North Atlantic in the 1920s. *J. Climate Appl. Meteor.,* **24,** 1303–1310.

——, 1990: Patterns of low frequency monthly sea-level pressure variability (1899–1986) and associated wave cyclone frequencies. *J. Climate,* **3,** 1364–1379.

——, and H. van Loon, 1979: The seesaw in winter temperature between Greenland and northern Europe. Part II: Some oceanic and atmospheric effects in middle and high latitudes. *Mon. Wea. Rev.,* **107,** 509–519.

Thompson, D. W. J., and J. M. Wallace, 1998: The Arctic oscillation signature in the wintertime geopotential height and temperature fields. *Geophys. Res. Lett.,* **25,** 1297–1300.

——, and ——, 2000a: Annular modes in the extratropical circulation. Part I: Month-to-month variability. *J. Climate,* **13,** 1000–1016.

——, and ——, 2000b: Annular modes in the extratropical circulation. Part II: Trends. *J. Climate,* **13,** 1018–1036.

van Loon, H., and J. C. Rogers, 1978: The seesaw in winter temperatures between Greenland and northern Europe. Part I: General description. *Mon. Wea. Rev.,* **106,** 296–310.

Walker, G. T., 1924: Correlation in seasonal variations of weather IX. Memo. India Meteorological Dept., 24, Part 9, 275–332.

Wallace, J. M., 2000: North Atlantic oscillation/annular mode: Two paradigms–one phenomenon. *Quart. J. Roy. Meteor. Soc.,* **126,** 791–805.

Woodruff, S., R. Slutz, R. Jenne, and P. Steurer, 1987: A Comprehensive Ocean–Atmosphere Data Set. *Bull. Amer. Meteor. Soc.,* **68,** 1239–1250.

Xie, S.-P., and Y. Tanimoto, 1998: A pan-Atlantic decadal climate oscillation. *Geophys. Res. Lett.,* **25,** 2185–2188.